Electronic Supplementary Information

Synthesis of diketopyrrolopyrrole and anthraquinone-based polymers of D-A1-D-A2 architecture by direct arylation polycondensation and designing inorganic/organic nano-heterostructured photoanodes for visible light water splitting

Mr. Nani Gopal Ghosh[†], Dr. Ayan Sarkar[†]*, Mr. Chandan Kumar, Mr. Himadri Shekhar Karmakar, Mr. Devendra Mayurdhwaj Sanke, and Prof. Sanjio S. Zade*

Department of Chemical Sciences and Centre for Advanced Functional Materials, Indian Institute of Science Education and Research (IISER) Kolkata, Mohanpur, Nadia, West Bengal, PIN-741246, India.

† Authors contributed equally.

*Corresponding Authors: A. Sarkar (visit2ayan@gmail.com), S. S. Zade (sanjiozade@iiserkol.ac.in)

Contents

Materials and reagents S3
Materials and reagents for organic synthesis S3
Materials and reagents for inorganic synthesis S3
Material syntheses S3
Monomer syntheses S3
1,5-bis [(2-ethylhexyl)oxy]-2,6-diiodoanthracene-9, 10- dione (2) S3
1, 5-bis((2-ethylhexyl)oxy)-4,8-di(thiophen-2-yl)anthracene-9,10-dione (4) S4
4,8-bis(5-bromothiophen-2-yl)-1,5-bis((2-ethylhexyl)oxy)anthracene-9,10-dione (5) S5
Polymer syntheses S5
Synthesis of PAQTDPP S5
Synthesis of PAQBTDPP S6
Synthesis of nitrogen-doped TiO_2 nanorods (N-TiO_2 NRs) S6
Fabrication of N-TiO_2/PAQTDPP and N-TiO_2/PAQBTDPP NHs S6
General measurements and characterizations S7
Characterizations for the organic materials S7
Characterization for the inorganic and inorganic/organic nano-hybrid materials S7
Photoelectrochemical measurements S8
Supplementary results and discussion S9
TGA and DSC thermograms S9
Crystallographic information S10
FTIR results S11
NMR Spectra S13
Theoretical Calculation S17
FESEM micrographs of NHs samples used for stability test S19
Water oxidation onset potential S19
Additional impedance studies S20
Comparison of the performances of the present electrodes with the other inorganic/organic hybrid photoanodes S21
PL studies S22
References S24

Materials and reagents

Materials and reagents for organic synthesis

All the reactions were done under a nitrogen environment to maintain dry conditions. Toluene and THF (tetrahydrofuran) were distilled from sodium/benzophenone wire before use. 1,5-dihydroxyanthraquinone (anthrarufin), *o*-phenylenediamine, thiophene, tributyltinchloride (Bu_3SnCl), tetrakis(triphenylphosphine)palladium(0) ($Pd(PPh_3)_4$), tris(dibenzylideneacetone)dipalladium(0)-chloroform adduct ($Pd_2(dba)_3{\cdot}CHCl_3$), tris(o-tolyl)phosphine ($P(o\text{-tol})_3$), triphenylphosphine (PPh_3), and $TBAPF_6$ were acquired from Aldrich and used without further purification. Iodine and iodic acid were purchased from Merck and Aldrich, respectively, and used without further purification. *n*-BuLi (1.6 M in hexane) was bought from Spectrochem.

Materials and reagents for inorganic synthesis

Titanium (IV) butoxide ($Ti(OBu)_4$, Sigma-Aldrich, 97% assay), fluorine-doped tin oxide (FTO) coated glass substrate (~7 Ohm/Sq., Sigma-Aldrich), hydrochloric acid (HCl 37%, Merck India), ammonia solution (28-30%, Merck India), deionized water (DI water, Merck Millipore).

Material syntheses

Monomer syntheses

3,6-di(thiophen-2-yl)-2,5-dihydropyrrolo[3,4-c]pyrrole-1,4-dione, 2,5-bis(2-ethylhexyl)-3,6-di(thiophen-2-yl)-2,5-dihydropyrrolo[3,4-c]pyrrole-1,4-dione (**3**)[1] 1,5-bis((2-ethylhexyl)oxy) anthracene-9,10-dione (**1**)[2] were synthesized according to the previously reported procedure.

1,5-bis [(2-ethylhexyl)oxy]-2,6-diiodoanthracene-9, 10- dione (2)

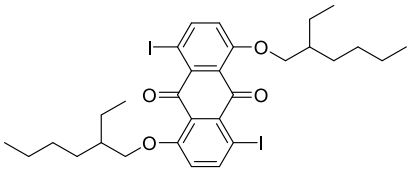

To a stirred solution of 1, 5-di O-(2-ethylhexyloxy)-anthraquinone (464 mg, 1 mmol) in 10 ml AcOH, NIS (450 mg, 2 mmol), TfOH (300 mg 2.0 mmol), were added. Subsequently, it was stirred at rt for 12 h. Then 10 ml of a saturated solution of $Na_2S_2O_3$ was added to the reaction mixture. AcOH in the reaction mixture was neutralized by a saturated solution of $NaHCO_3$. The reaction mixture was extracted with 3×20 ml ethyl acetate, and it was recrystallized from DCM/EtOH mixture in 98% yield (702 mg).

^{1}H NMR: (400MHz, $CDCl_3$): δ = 8.02 (d, *J* = 9.0Hz, 2H), 6.85 (d , *J* = 8.9Hz, 2H), 3.96 (m, 4H), 1.82-1.34 (m, J = 7 Hz, 16H), 0.92(t, *J* = 7Hz, 6H).

^{13}C NMR (101 MHz, CHLOROFORM-D) δ 182.81, 158.43, 149.07, 146.57, 138.37, 124.85, 78.99, 72.03, 44.94, 39.51, 30.51, 29.26, 23.89, 23.24, 14.28, 11.40.

HRMS: (ESI) Calculated for $C_{30}H_{38}O_4I_2$ $[M+H]^+$ calculated 717.08, found 717.09.

1, 5-bis((2-ethylhexyl)oxy)-4,8-di(thiophen-2-yl)anthracene-9,10-dione (4)

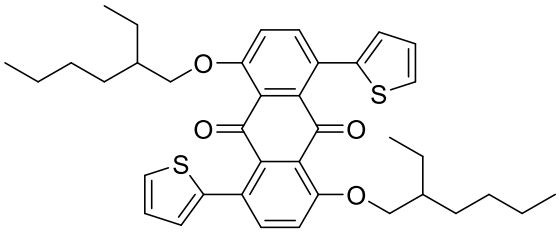

To a stirred deoxygenated solution of 1,5-bis((2-ethylhexyl)oxy)-4,8-diiodoanthracene-9,10-dione (2 g, 2.79 mmol) and tributyl(thiophene-2-yl)stannane (4.4 g, 11.53 mmol) in 40 ml toluene, $Pd(PPh_3)_4$ (400 mg, 0.27 mmol) was added under nitrogen atmosphere and the reaction mixture was purged with N_2 for 10 min. It was then heated to 110 °C for 24 h. After that, the reaction mixture was cooled down to room temperature (RT), and toluene was removed under reduced pressure. A saturated solution of KF was added to the reaction mixture. The reaction mixture was extracted with 3×20 ml ethyl acetate and dried over Na_2SO_4. The solvent was removed under reduced pressure; it was purified by 2-5% ethyl acetate in hexane to give as a reddish-yellow solid (1.5 g, 85%).

^{1}H NMR (400 MHz, Chloroform-d) δ 7.57 (d, *J* = 8.8 Hz, 2H), 7.32 (d, *J* = 4.1 Hz, 2H), 7.12 (d, *J* = 8.9 Hz, 2H), 7.06 (d, 2H), 7.06 – 7.03 (m, 2H), 3.98 (m, 4H), 1.77 (m, 2H), 1.57 (m, 2H), 1.46 (m, 4H), 1.33 (m, 8H), 0.92 (m, 12H).

^{13}C NMR (101 MHz, Chloroform-d) δ 184.92, 157.34, 141.26, 137.30, 127.18, 125.60, 125.20, 124.58, 115.94, 71.36, 39.38, 30.34, 29.29, 23.68, 23.20, 14.36, 11.30.

HRMS: (ESI) Calculated for $C_{38}H_{44}O_4S_2$ $[M+Na]^+$ 651.2573, found 651.2556.

4,8-bis(5-bromothiophen-2-yl)-1,5-bis((2-ethylhexyl)oxy)anthracene-9,10-dione (5)

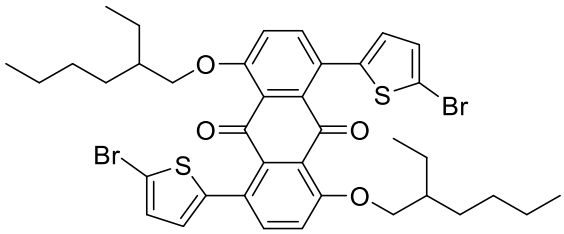

Compound **4** (0.76 g, 2.71 mmol) was dissolved in chloroform (15 ml), and then NBS (1.01 g, 5.69 mmol) was added portion-wise to it in dark condition at RT. After 4 h of stirring at RT, water was added to the reaction mixture. The reaction mixture was extracted with 3×20 ml chloroform and dried over Na_2SO_4. The solvent was removed under reduced pressure, and then the compound was purified by silica gel column chromatography with ethyl acetate/hexane 2-5% to obtain compound **5** as a greenish-yellow (1.1 g, 88%) solid.

^{1}H NMR (400 MHz, Chloroform-d) δ 7.51 (d, *J* = 8.9 Hz, 2H), 7.12 (d, *J* = 8.8 Hz, 2H), 6.99 (d, *J* = 3.8 Hz, 2H), 6.82 (d, *J* = 3.7 Hz, 2H), 3.98 (m, 2H), 1.76 (s, 1H), 1.46 (s, 3H), 1.32 (s, 5H), 0.91 (s, 6H).

^{13}C NMR (101 MHz, Chloroform-d) δ 184.59, 157.74, 142.80, 137.37, 129.92, 127.49, 124.45, 124.30, 116.13, 112.40, 71.43, 39.29, 29.29, 29.19, 23.71, 23.19, 14.36, 11.28.

HRMS: (ESI) Calculated for $C_{38}H_{42}O_4S_2Br_2$ $[M]^+$ 786.09.

Polymer syntheses

Synthesis of PAQTDPP

1,5-bis((2-ethylhexyl)oxy)-4,8-diiodoanthracene-9,10-dione (**2**) (123.2 mg, 0.2 mmol) and 2,5-bis(2-ethylhexyl)-3,6-di(thiophene-2-yl)-2,5-dihydropyrrolo[3,4-c]pyrrole-1,4-dione (**3**) (105 mg, 0.2 mmol), $Pd_2(dba)_3{\cdot}CHCl_3$ (9.15 mg, 4.4 mol%), P(*o* -MeOPh)$_3$ (12.5mg, 8.8 mol%), pivalic acid (20.5 mg, 0.20 mmol), and Cs_2CO_3 (195 mg, 0.60 mmol) were added in a round bottom flask with a condenser and a magnetic stirring bar under nitrogen atmosphere. Then 5 ml degassed toluene was added to the reaction mixture. The mixture was heated to 120 °C under magnetic stirring for 24 h. After cooling to room temperature, the mixture was precipitated in methanol. The crude polymer was collected by filtration and purified by Soxhlet extraction with acetone, hexane, and chloroform successively. The chloroform solution was concentrated and was reprecipitated into methanol. Yield: 92% (154 mg).

.

Synthesis of PAQBTDPP

4,8-bis(5-bromothiophen-2-yl)-1,5-bis((2-ethylhexyl)oxy)anthracene-9,10-dione (**3**) (250 mg, 0.317 mmol) and 2,5-bis(2-ethylhexyl)-3,6-di(thiophene-2-yl)-2,5-dihydropyrrolo[3,4-c]pyrrole-1,4-dione (**1**) (167 mg, 0.317 mmol), $Pd_2(dba)_3 \cdot CHCl_3$ (14.5 mg, 0.014 mmol), P(*o* -MeOPh)$_3$ (11.11 mg, 0.0315 mmol), pivalic acid (32.5 mg, 0.317 mmol), and Cs_2CO_3 (310 mg, 0.95 mmol) were added in a round bottom flask with a condenser with a magnetic stirring bar under nitrogen atmosphere. Then 5 ml degassed toluene was added to the reaction mixture. The mixture was heated to 120 °C under magnetic stirring for 24 h. After cooling to room temperature, the mixture was precipitated in methanol. The crude polymer was collected by filtration and purified by Soxhlet extraction with acetone, hexane, and chloroform successively. The chloroform solution was concentrated and was reprecipitated into methanol. Yield: 85.2% (298 mg).

Synthesis of nitrogen-doped TiO_2 nanorods (N-TiO_2 NRs)

At first, pristine rutile TiO_2 NRs were grown on the FTO coated glass substrate, as described in our previous publication.[2] Briefly, 0.3 ml $Ti(OBu)_4$ was slowly drop-casted into a solution of 8 ml DI water and 8 ml HCl under magnetically stirring conditions, and the solution was further stirred for another 20 min. Then previously cleaned FTO substrates (1×2 cm^2) were inserted into a 25 ml Teflon-lined vessel in tilted condition with the FTO coated surface facing upward. A suitable amount of the titanium precursor solution was poured into the vessel. The vessel was placed inside of a stainless steel autoclave and heated at 150 °C for 4 h. After natural cooling, the FTO substrates were properly cleaned by ethanol, isopropanol, and water and dried.

The nitrogen doping in TiO_2 was achieved by soaking TiO_2 in an ammonia solution, followed by annealing in an argon atmosphere.[3] The as-prepared TiO_2/FTO samples were vertically attached inside a closed glass vessel, and only the TiO_2 containing part of the FTO substrate was dipped in a 28-30% ammonia solution for 24 h. The remaining conducting part surface of the FTO coated substrate was masked with Teflon tape. After 24 h, the samples were rinsed with water and ethanol and dried with tissue paper. Finally, the samples were annealed at 450 °C for 2 h under argon gas flow.

Fabrication of N-TiO_2/PAQTDPP and N-TiO_2/PAQBTDPP NHs

The N-TiO_2/PAQTDPP and N-TiO_2/PAQBTDPP NHs thin films were fabricated using the simple spin-coating technique. Firstly, two different solutions of PAQTDPP and PAQBTDPP polymers were prepared by dissolving 5 mg of the respective polymers in 1 ml $CHCl_3$. For

preparing N-TiO_2/PAQTDPP NHs, the surface of the N-TiO_2/FTO sample was properly drenched by drop-casting the freshly prepared PAQTDPP solution, and then the N-TiO_2/FTO sample was spun at 3000 rpm for 15 s in a spin-coater. Lastly, the spin-coated samples were annealed at 100 °C under nitrogen gas flow for 1 h inside a conical flask, placed inside a silicone oil bath. The same method was followed to fabricate the N-TiO_2/PAQBTDPP NHs thin films, except the PAQBTDPP solution was used instead of the PAQTDPP solution.

General measurements and characterizations

Characterizations for the organic materials

^{1}H nuclear magnetic resonance (NMR) and ^{13}C NMR spectra were recorded using a JEOL ECS 400 MHz and Bruker AVANCE 500 MHz spectrometer with $CDCl_3$ or DMSO-d_6 as the solvent, and chemical shifts (δ) are reported in parts per million (ppm) relative to tetramethylsilane as the standard internal values. The coupling constants (J) are given in Hz. The apparent resonance multiplicity is described as s (singlet), br s (broad singlet), d (doublet), t (triplet), q (quartet), and m (multiplet).

Characterization for the inorganic and inorganic/organic nano-hybrid materials

The structure and morphology of the as-prepared N-TiO_2 NRs, N-TiO_2/PAQTDPP NHs, and N-TiO_2/PABQTDPP NHs were studied by a field-emission electron microscope (FESEM, Zeiss SUPRA 55-VP). An atomic force microscope (AFM, Ntegra Prima, NT-MDT Spectrum Instruments) was used to probe the topography of the materials. Thermogravimetric analysis (TGA) and Differential scanning calorimetry (DSC) were done using the Mettler Toledo instruments. The X-ray diffraction (XRD) patterns of the N-TiO_2 NRs, N-TiO_2/PAQTDPP NHs, N-TiO_2/PABQTDPP NHs, and polymer powders were recorded using a Rigaku MiniFlex diffractometer, where a Cu K_α line (λ = 1.54 Å) was used as the X-ray source. Solid-state room temperature UV-Vis-NIR absorption spectra of all the materials were recorded using an Agilent Cary 3500 spectrophotometer. The room temperature solid-state photoluminescence spectra of all the materials were recorded utilizing a Horiba Fluoromax 4 Spectrofluorometer (excitation wavelength 325 nm). Monochromatic X-ray photoelectron spectroscopy (XPS, Kratos Analytical, AXIS Supra, Al anode) was also used to analyze the constituent elements and their ionic states of the N-TiO_2/PAQTDPP NHs sample. The polymers' Fourier transform infrared (FTIR) spectra were taken using the Perkin-Elmer Spectrum Two FT-IR spectrometer. After the 1 h photostability tests, the polymers were taken out of the NHs by dissolving in $CHCl_3$ and were used for FTIR analysis. The time-resolved photoluminescence (TRPL) studies were executed employing the time-correlated single-photon counting (TCSPC) method utilizing a picosecond spectrofluorometer (Horiba Jobin Yvon IBH equipped with a FluoroHub single-

photon counting controller). The NHs samples were scratched off the FTO substrates and dispersed in DI water. The dispersion was excited by a 375 nm diode laser, and the emission decay at 410 nm was recorded in each case. The TRPL spectra of the two polymers were recorded using their $CHCl_3$ solutions. The polymers were excited at their respective absorption maxima, and the decay was recorded at the emission maxima.

Photoelectrochemical measurements

The photoelectrochemical measurements were carried out using a three-electrode electrochemical workstation (CH Instruments, CHI 608D) inside a standard electrochemical cell. The samples (prepared on FTO substrate) served as the working electrode, a Pt wire as the counter electrode, and an Ag/AgCl (saturated in 1 M aq. KCl) as the reference electrode. A 0.5 M aq. Na_2SO_4 solution (pH~ 6.7) was used as the electrolyte for all the measurements unless another electrolyte is explicitly mentioned.

The linear sweep voltammetry (LSV) measurements ranged from -1 $V_{Ag/AgCl}$ to 1 $V_{Ag/AgCl}$ at 10 mV/s. The Mott-Schottky measurements were performed by running the impedance-potential program at 1 kHz in the range of -1 $V_{Ag/AgCl}$ to 1 $V_{Ag/AgCl}$. The electrochemical impedance spectroscopy (EIS)-related measurements were performed by executing the AC impedance from 1 MHz to 0.1 Hz at 0 $V_{Ag/AgCl}$ (DC) with 5 mV AC perturbation.

A Newport Xe lamp with AM 1.5G filter and adjusted light intensity of 100 mW/cm^2 was used as the light source.

Using the following formula, the potential measured against the Ag/AgCl reference electrode has been converted against the reversible hydrogen electrode (RHE).

$$V_{RHE} = V_{Ag/AgCl} + 0.059 \times pH + V^0_{Ag/AgCl}$$

Here, $V^0_{Ag/AgCl} = 0.1976$ V at 298 K in saturated KCl.

The amount of photoelectrochemically produced hydrogen gas and oxygen gas were collected separately (as shown in Figure S1) using a graduated inverted burette, keeping the other experimental parameter the same under visible light illumination from a 100 W Xe lamp intensity of 100 mW/cm^2. Oxygen was collected at the working electrode (WE, NHs photoanode), while hydrogen was collected at the counter electrode (CE, Pt wire).

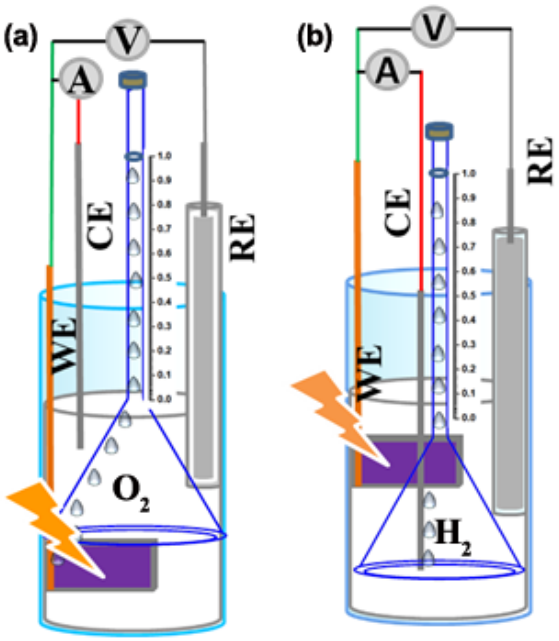

Figure S1: Schematic diagrams of the inverted-burette arrangments to collect photoelectrochemically generated (a) O_2 and (b) H_2.

Supplementary results and discussion

TGA and DSC thermograms

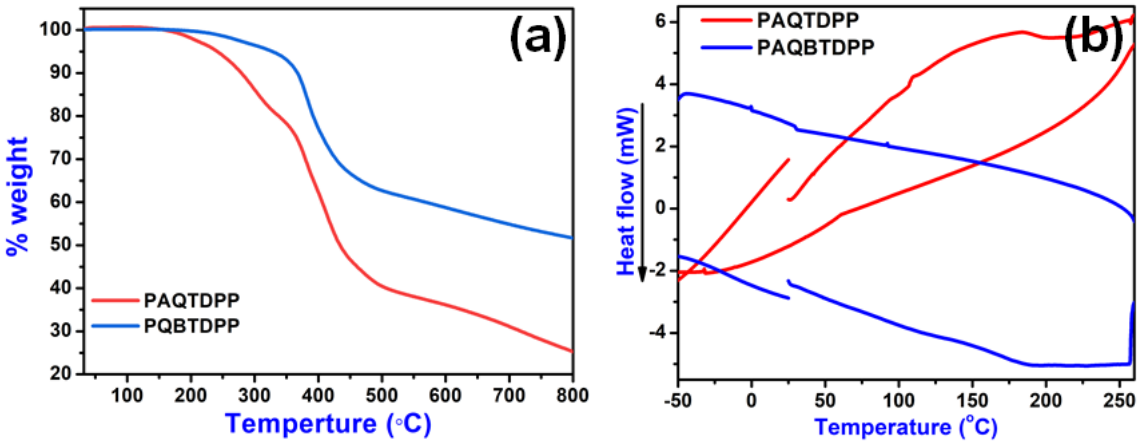

Figure S2: The (a) TGA and (b) DSC thermograms of PAQTDPP and PAQBTDPP polymers.

Crystallographic information

Table S1: Crystallographic data of Compound **2**.

Identification code	Compound **2**
Empirical formula	$C_{22}H_{22}I_2O_4$
Formula weight	604.20
Temperature/K	100.00(10)
Crystal system	orthorhombic
Space group	Fdd2
a/Å	10.4919(3)
b/Å	27.9599(10)
c/Å	14.2253(5)
α/°	90.00
β/°	90.00
γ/°	90.00
Volume/Å^3	4173.0(2)
Z	8
ρ_{calc}g/cm^3	1.923
μ/mm^{-1}	23.888
F(000)	2336.0
Crystal size/mm^3	0.04 × 0.02 × 0.005
Radiation	Cu Kα (λ = 1.54184 Å)
2Θ range for data collection/°	10.94 to 132.48
Index ranges	$-12 \leq h \leq 12$, $-33 \leq k \leq 32$, $-16 \leq l \leq 13$
Reflections collected	7724
Independent reflections	1677 [R_{int} = 0.0385, R_{sigma} = 0.0247]
Data/restraints/parameters	1677/1/128
Goodness-of-fit on F^2	1.047
Final R indexes [I>=2σ (I)]	R_1 = 0.0411, wR_2 = 0.1036
Final R indexes [all data]	R_1 = 0.0411, wR_2 = 0.1037
Largest diff. peak/hole / e Å^{-3}	1.04/-1.26
Flack parameter	0.001(10)
CCDC number	2099189

FTIR results

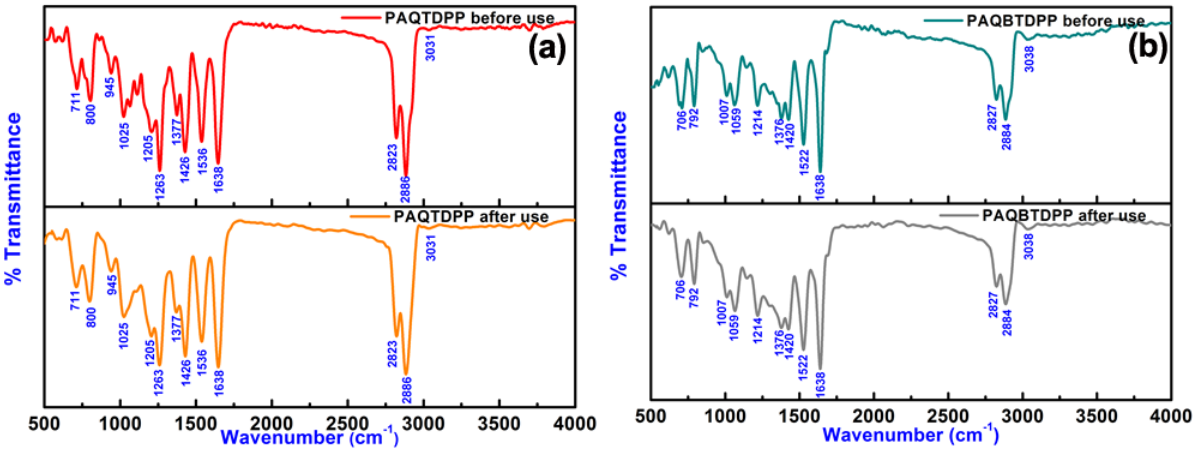

Figure S3: FTIR (ATR) spectra of (a) PAQTDPP and (b) PAQBTDPP polymers before use and after a 1 h stability test.

Table S2: FTIR analysis of PAQTDPP.

Group	Wavenumber (cm^{-1})	Intensity	Ref.
sp^2 C–H stretch (aromatic)	3031	Weak	1
sp^3 C–H stretch (aliphatic)	2886	Strong	1
sp^3 C–H stretch (aliphatic)	2823	Strong	1
C=O stretching (longer conjugated system)	1638	Strong	1
C=C stretching (aromatic)	1536	Medium	1
C-N stretch	1426	Strong	1
sp^3 C-H bending (aliphatic)	1377	Medium	1
sp^2 C-O stretching (tutomeric =C-O^-)	1263	strong	1
sp^3 C-C stretch	1200	Medium	1
sp^3 C-O stretch	1025	Medium	1
sp^2 C-H bending (out of plane)	941	Medium	1
sp^2 C=C stretch (para di-substituted aromatic ring)	800	Medium	1
sp^3 CH_2 bending in-plane (rocking)	711	Medium	1

Table S3: FTIR analysis of PAQBTDPP.

Group	Wavenumber (cm^{-1})	Intensity	Ref.
sp^2 C–H stretch (aromatic)	3038	Weak	1
sp^3 C–H stretch (aliphatic)	2884	Strong	1
sp^3 C–H stretch (aliphatic)	2827	Strong	1
C=O stretching(longer conjugated system)	1638	Strong	1
C=C stretching (aromatic)	1522	Strong	1
C-N stretch	1420	Strong	1
sp^3 C-H bending (aliphatic)	1376	Strong	1
sp^3 C-C stretch	1200	Medium	1
sp^3 C-O stretch	1059	Medium	1
sp^2 C-H bending (out of plane)	1007	Medium	1
sp^2 C=C stretch (para di-substituted aromatic ring)	792	Medium	1
sp^3 CH_2 bending in-plane (rocking)	706	Medium	1
sp^2 C-H out of plane bending (aromatic)	620	Weak	1

NMR Spectra

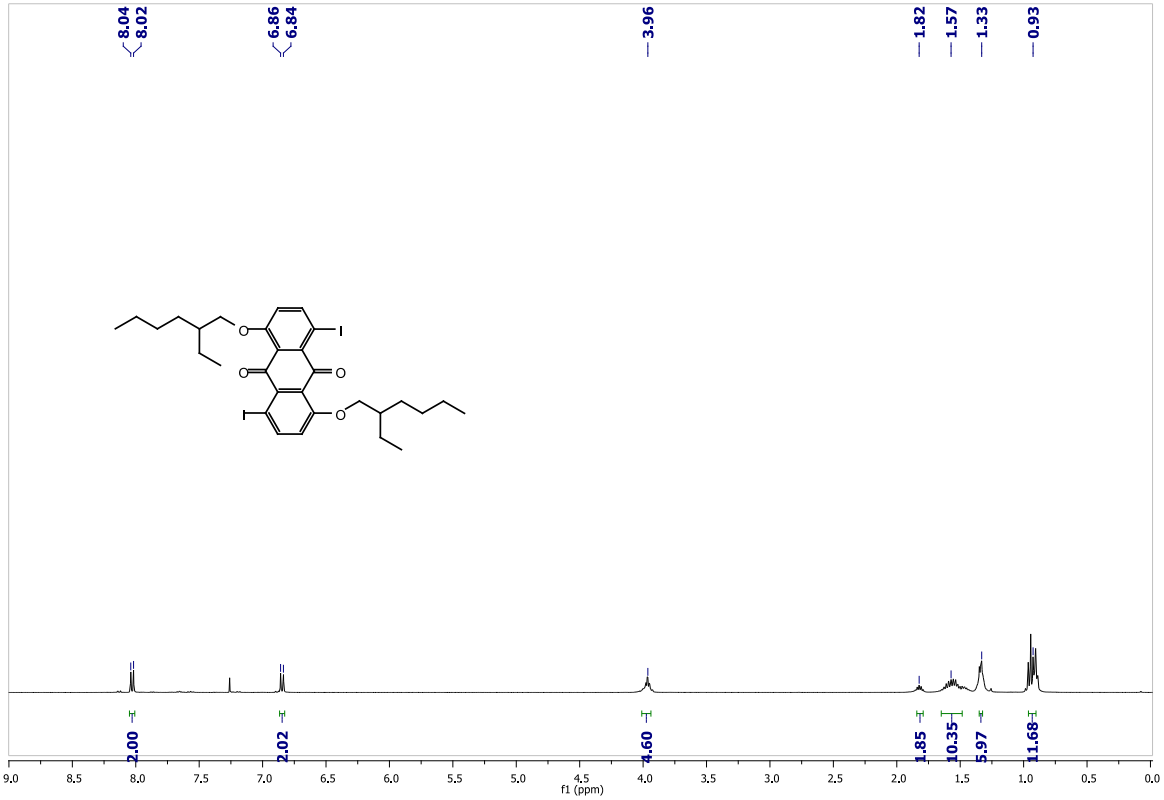

Figure S4: ^{1}H NMR spectra of compound **6**.

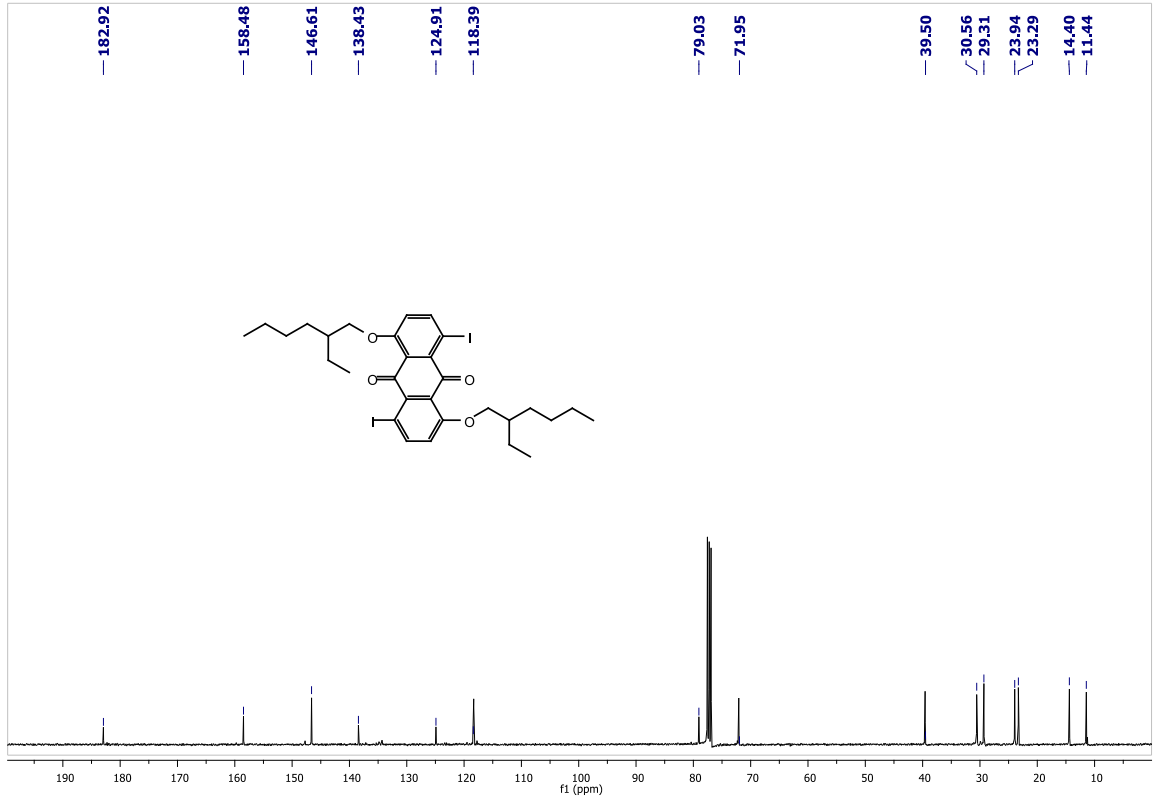

Figure S5: ^{13}C NMR spectra of compound **6**.

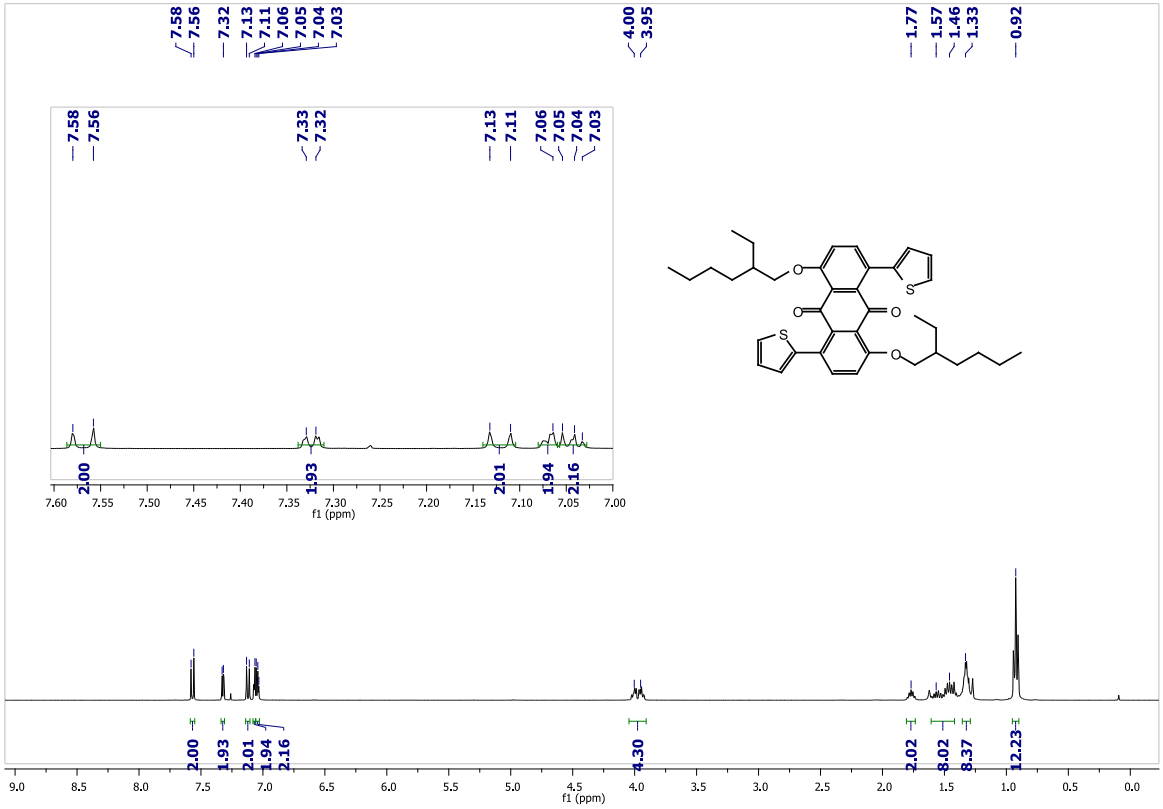

Figure S6: ^{1}H NMR spectra of compound **6**.

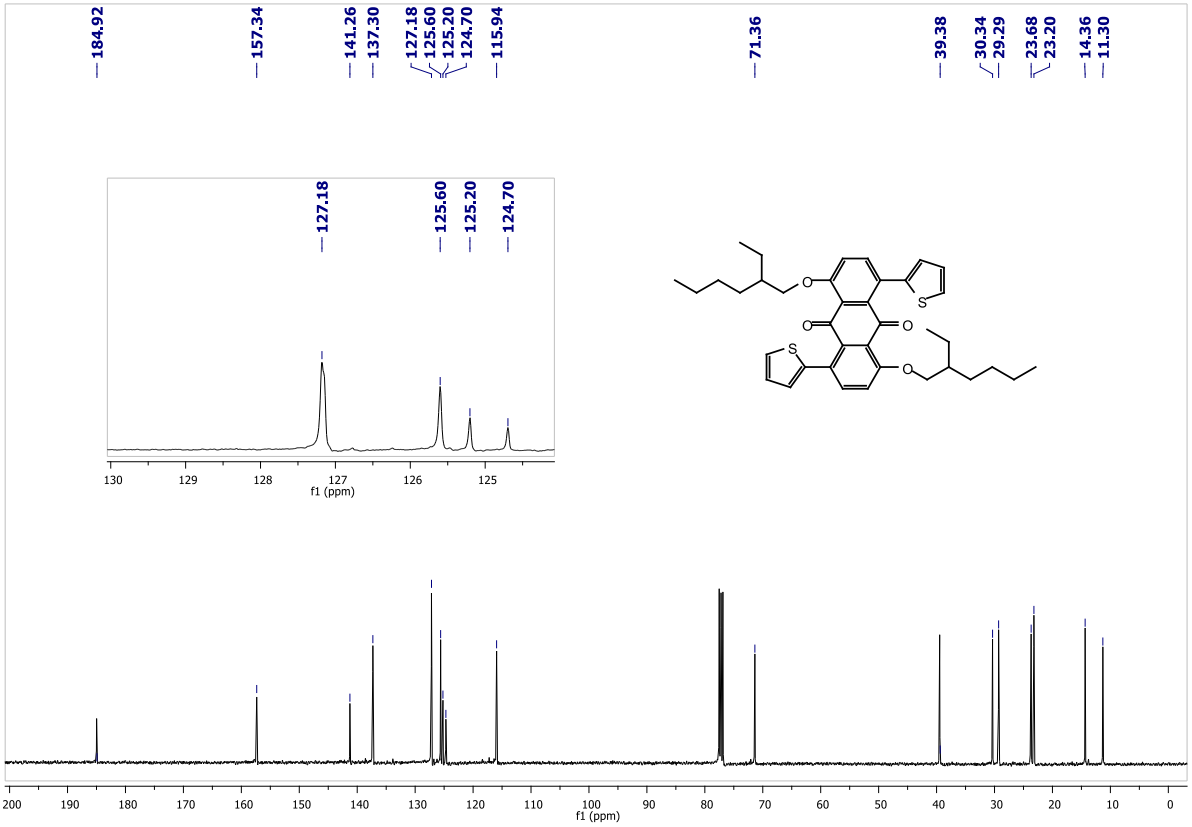

Figure S7: ^{13}C NMR spectrum of compound **5**.

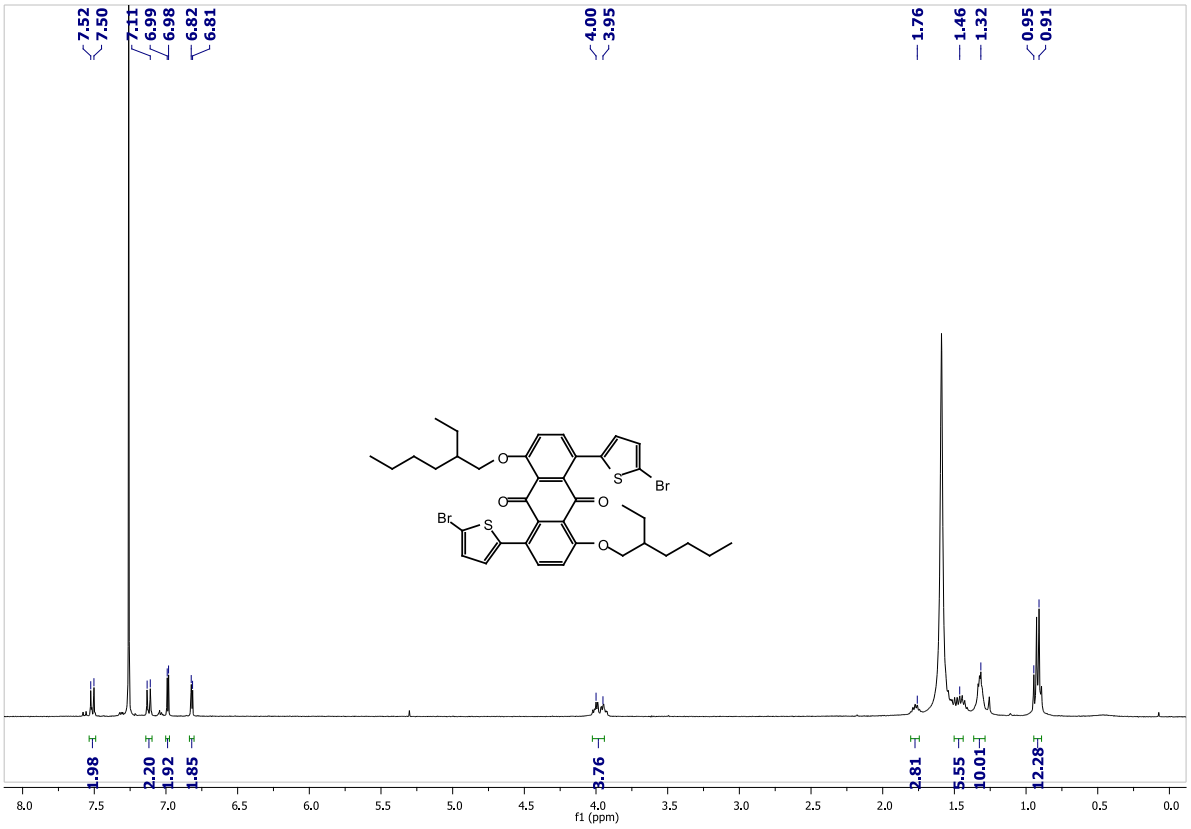

Figure S8:^{1}H NMR spectra of compound **7**.

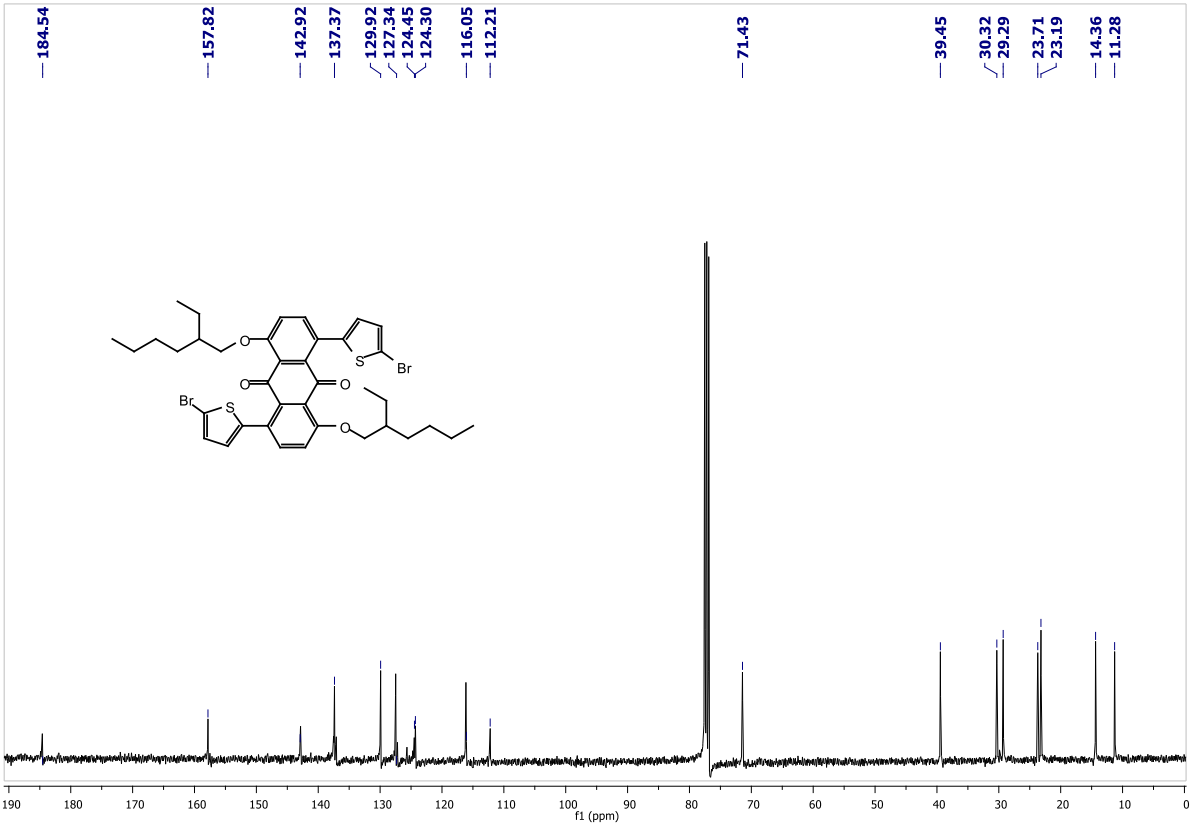

Figure S9: ^{13}C NMR spectra of compound **7**.

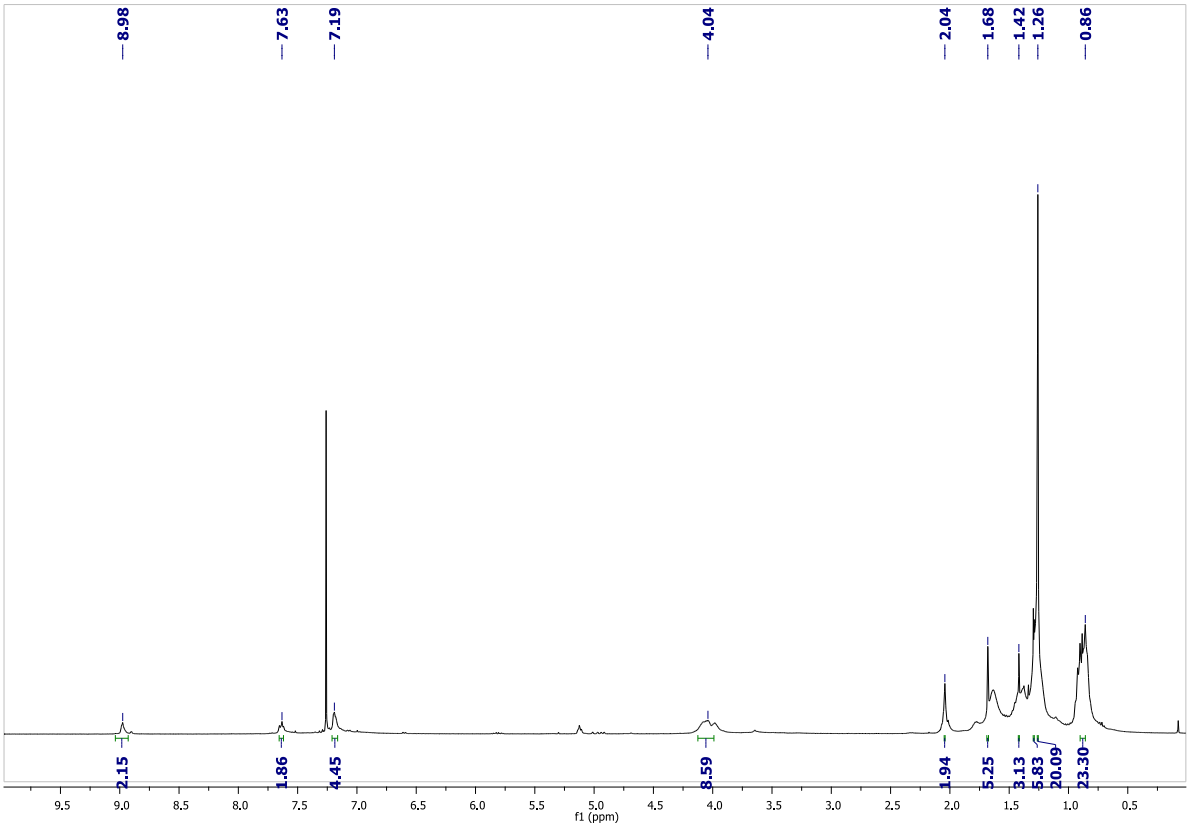

Figure S10: ^{1}H NMR spectra of PAQTDPP.

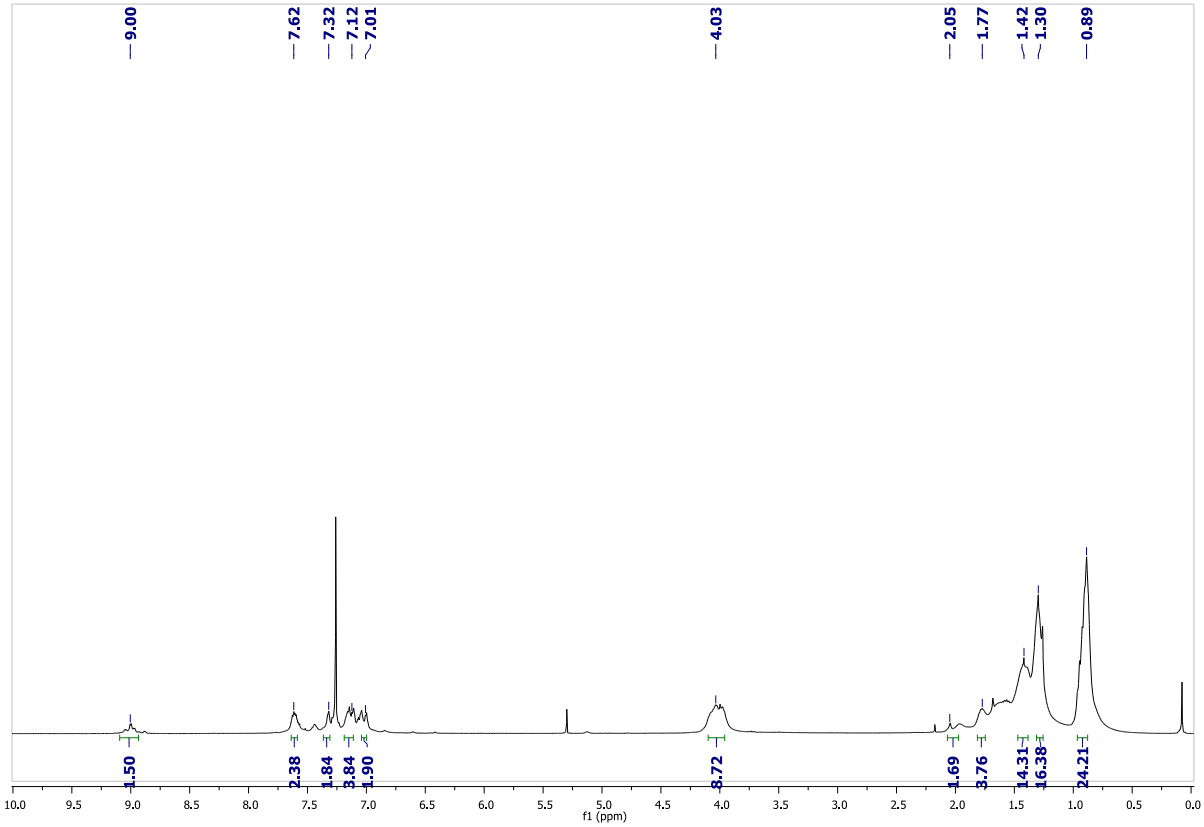

Figure S11: ^{1}H NMR spectra of PAQBTDPP.

Theoretical Calculation

The HOMO (highest occupied molecular orbital) and LUMO (lowest unoccupied molecular orbital) coefficients of PAQTDPP and PAQBTDPP were calculated via DFT calculation at B3LYP/6-31G(d) using the Gaussian 16 package. The HOMO and LUMO diagrams of PAQTDPP and PAQBTDPP are given in Figure S12. Using those optimized structures of PAQTDPP and PAQBTDPP, the time-dependent density-functional theory (TDDFT) calculations were performed at B3LYP/6-31G(d) to predict their theoretical UV-Vis-NIR spectra (Figure S13).

Table S4: Major Orbital contribution of absorption spectra of PAQTDPP and PAQBRDPP.

	Ground State	Excited State	oscillator strength
PAQTDPP at 587 nm	HOMO-1	LUMO+2	0.68377
	HOMO-1	LUMO+4	0.10761
	HOMO	LUMO+2	0.11060
PAQBTDPP at 617 nm	HOMO	LUMO	0.21456
	HOMO	LUMO+1	0.12624
	HOMO	LUMO+2	0.49326
	HOMO	LUMO+3	0.42773

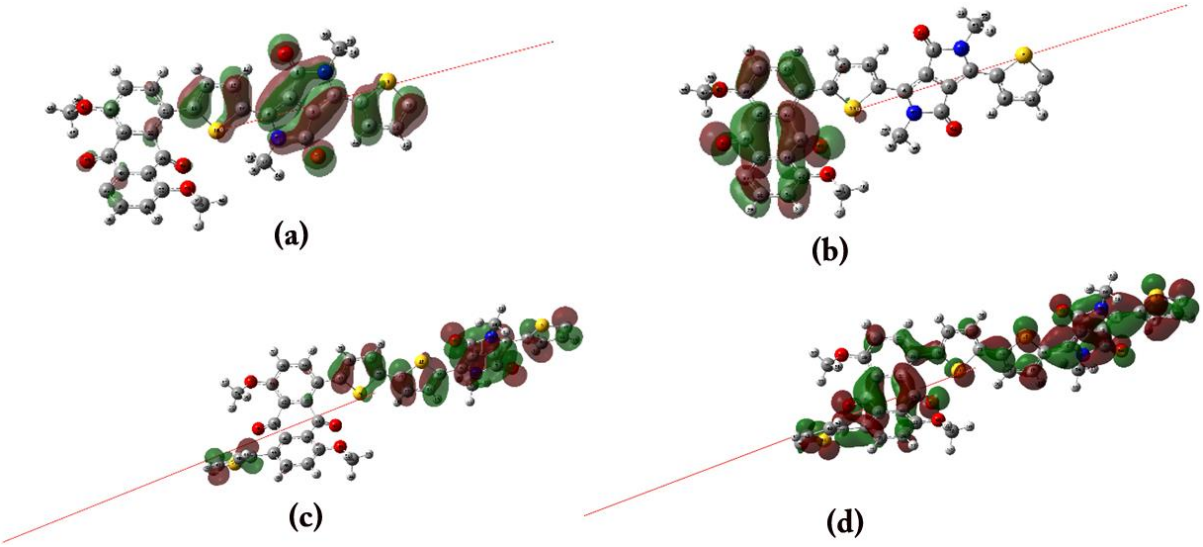

Figure S12: HOMO representation of (a) PAQTDPP and (c) PAQBTDPP. LUMO representation of (b) PAQTDPP and (d) PAQBTDPP.

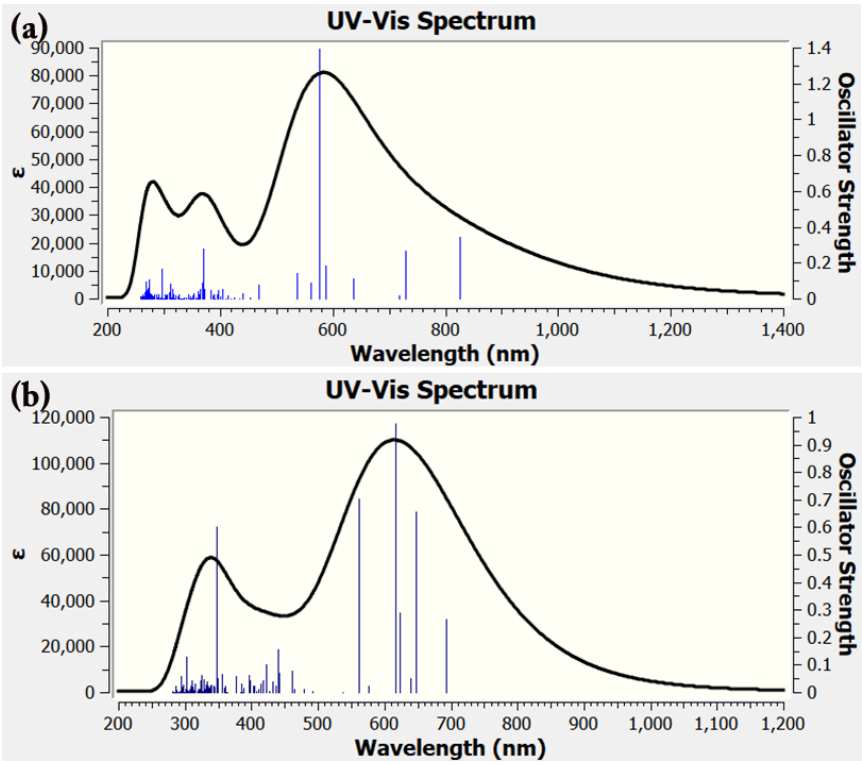

Figure S13: Theoretically predicted UV-Vis-NIR spectra of the (a) PAQTDPP and (b) PAQBTDPP polymers.

FESEM micrographs of NHs samples used for stability test

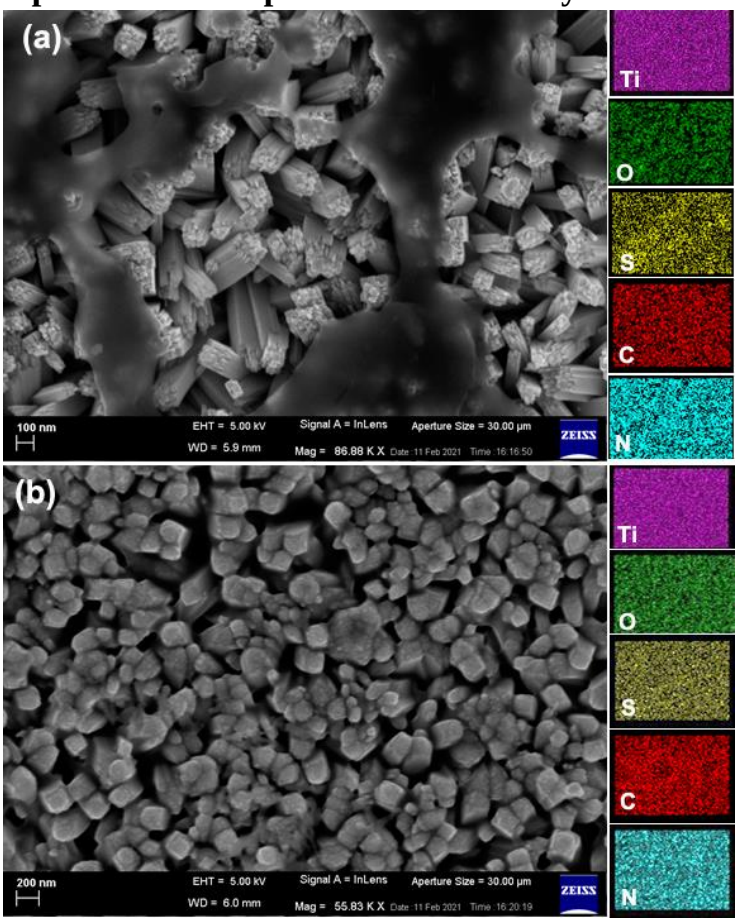

Figure S14: FESEM micrographs with corresponding EDS color mappings of (a) N-TiO_2/PAQTDPP NHs and (b) N-TiO_2/PAQBTDPP NHs, after 1 h stability test.

Water oxidation onset potential

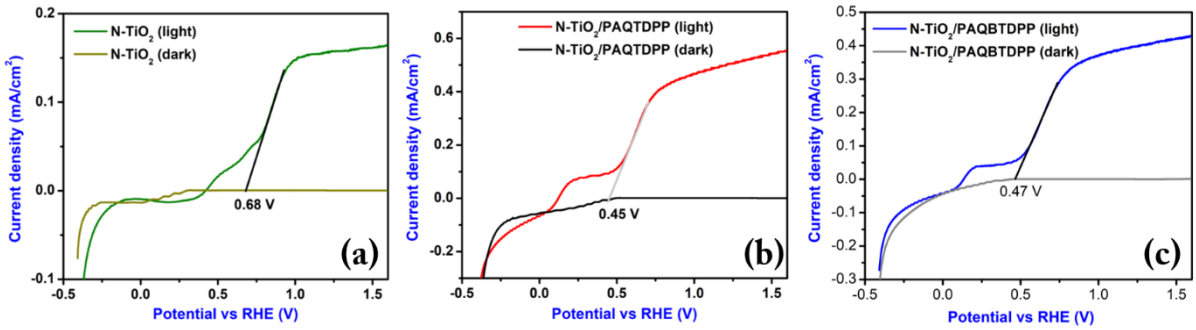

Figure S15: The current density vs. applied potential plots under dark and visible-light illuminated conditions for estimating the oxidation onset potential (V_{op}) of (a) N-TiO_2 NRs, (b) N-TiO_2/PAQTDPP NHs, and (c) N-TiO_2/PAQBTDPP NHs electrodes.

Additional impedance studies

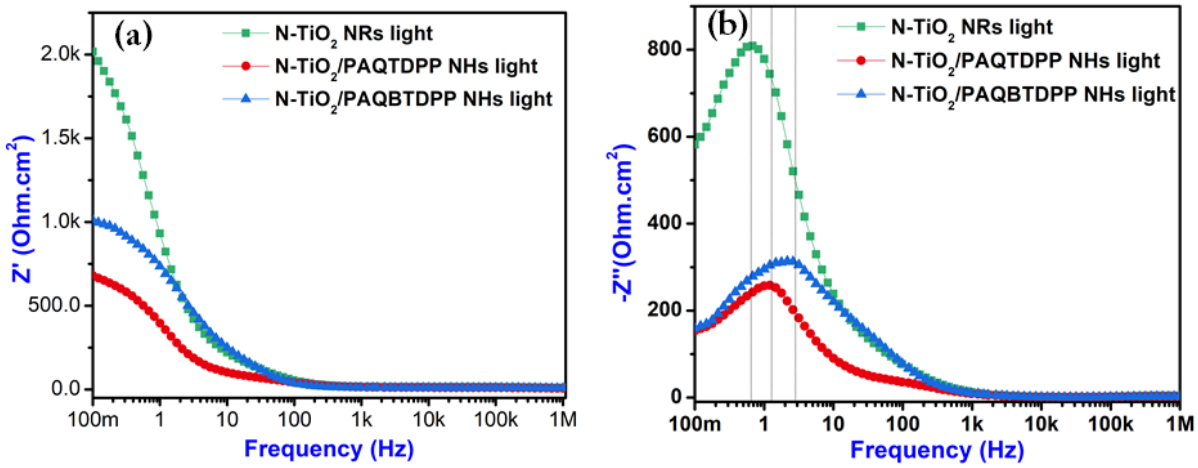

Figure S16: Room temperature (a) Z′ vs frequency plot (b) Z″ vs frequency plot for the three photoelectrodes.

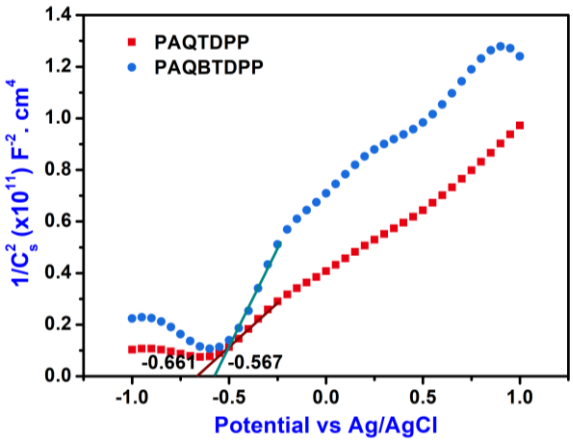

Figure S17: Mott-Schottky plots of PAQTDPP and PAQBTDPP polymers coated on FTO.

Comparison of the performances of the present electrodes with the other inorganic/organic hybrid photoanodes

Table S5: PEC performances of some reported inorganic/organic hetero-structured photoanodes.

Photoanode	Electrolyte	Photocurrent density J_{ph} (scan rate)	Maximum photoconversion efficiency%	Light intensity (mW/cm^2)
FTO/Ti^{3+}/TiO_2/P1[2]	0.5 M aq. Na_2SO_4	0.50 mA/cm^2 at 1.23 V_{RHE}. (10 mV/s)	0.26	100
FTO/Ti^{3+}/TiO_2/P2[2]	0.5 M aq. Na_2SO_4	0.28 mA/cm^2 at 1.23 V_{RHE}. (10 mV/s)	0.11	100
FTO/BBL/TiO_2/Ni-Co[4]	0.5 M aq. Na_2SO_4/ phosphate buffer (pH 7)	0.03 mA/cm^2 at 1.23 V_{RHE}. (10 mV/s)	NA	100
NiFe-MOF/TiO_2[5]	0.5 M aq. Na_2SO_4	0.77 mA/cm^2 at 1.23 V_{RHE}. (50 mV/s)	0.19	100
ITO/PMPDI/CoO_x [6]	0.1 M pH 7 KPi buffer	0.15 mA/cm^2 at 1 $V_{Ag/AgCl}$. (5 mV/s)	NA	100
ITO/ZnO/ $PC_{71}BM$[7]	0.1 M aq. KOH	0.06 mA/cm^2 at 1.23 V_{RHE}. (not mentioned)	NA	100
FTO/TiO_2/$RGO_{(0.1\%)}$[8]	0.5 M aq. H_2SO_4	0.2 mA/cm^2 at 1.23 V_{RHE}. (not mentioned)	NA	100
FTO/Fe_2O_3/Melanin[9]	80 mM phosphate (pH 7.5)	0.78 mA/cm^2 at 1.23 V_{RHE}. (not mentioned)	NA	100
$(TiO_2/BPEI/MoS_2)_2$[10]	0.5 M aq. Na_2SO_4	~0.3 mA/cm^2 at 1.23 V_{RHE}. (5 mV/s)	0.16	100
FTO/TiO_2/Au/Polythiophene[11]	0.5 M aq. Na_2SO_4	0.24 mA/cm^2 at 0.8 $V_{Ag/AgCl}$. (not mentioned)	0.11	50

Photoanode	Electrolyte	Photocurrent density J_{ph} (scan rate)	Maximum photoconversion efficiency%	Light intensity (mW/cm^2)
FTO/PANI-TiO_2[12]	0.1 M aq. NaOH	~0.01 mA/cm^2 at 1.23 V_{RHE}. (10 mV/s)	NA	100
FTO/B-TiO_2/NDIEHTh@Au-Pd [13]	0.5 M aq. Na_2SO_4	1.09 mA/cm^2 at 1.23 V_{RHE}. (10 mV/s)	0.32	100
FTO/N-TiO_2/PAQTDPP (This work)	0.5 M aq. Na_2SO_4	0.504 mA/cm^2 at 1.23 V_{RHE} (10 mV/s)	0.19	100
FTO/N-TiO_2/PAQBTDPP (This work)	0.5 M aq. Na_2SO_4	0.397 mA/cm^2 at 1.23 V_{RHE} (10 mV/s)	0.12	100

PL studies

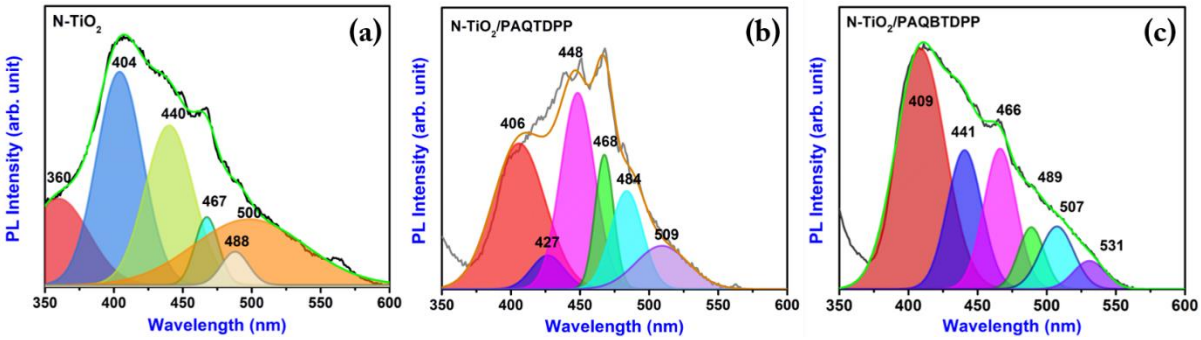

Figure S18: Gaussian curve-fitted PL spectra of (a) N-TiO_2 NRs, (b) N-TiO_2/PAQTDPP NHs, and (c) N-TiO_2/PAQBTDPP NHs.

Table S6: FWHM values of different Gaussian peaks of the deconvoluted PL spectra shown in Figure S18.

	Peak Position (nm)	FWHM (nm)
N-TiO_2 NRs	360	51.72
	404	39.25
	440	41.09
	467	20.27
	488	23.31
	500	95.46
N-TiO_2 /PAQTDPP NHs	406	44.75
	427	27.84
	448	28.91
	468	15.85
	484	27.15
	509	44.92
N-TiO_2 /PAQBTDPP NHs	409	41.78
	441	29.44
	466	27.63
	489	22.03
	507	28.50
	531	27.38

Table S7: Relevant data for calculating τ_{avg}

Compound	B_1	B_2	B_3	τ_1 (ns)	τ_2 (ns)	τ_3 (ns)	τ_{avg} (ns)
PAQTDPP	6.72×10^{-3}	4.08×10^{-2}	7.52×10^{-4}	0.44	0.91	3.68	0.886
PAQBTDPP	2.92×10^{-2}	1.92×10^{-2}	6.71×10^{-5}	0.74	0.93	5.06	0.824

References

[1] E. Heyer, R. Ziessel, *Synlett* **2015**, *26*, 2109.

[2] N. G. Ghosh, A. Sarkar, S. S. Zade, *Chem. Eng. J.* **2021**, *407*, 127227.

[3] A. Sarkar, K. Karmakar, A. K. Singh, K. Mandal, G. G. Khan, *Phys. Chem. Chem. Phys.* **2016**, *18*, 26900.

[4] P. Bornoz, M. S. Prévot, X. Yu, N. Guijarro, K. Sivula, *J. Am. Chem. Soc.* **2015**, *137*, 15338.

[5] W. Cui, H. Bai, J. Shang, F. Wang, D. Xu, J. Ding, W. Fan, W. Shi, *Electrochim. Acta* **2020**, *349*, 136383.

[6] J. T. Kirner, J. J. Stracke, B. A. Gregg, R. G. Finke, *ACS Appl. Mater. Interfaces* **2014**, *6*, 13367.

[7] L. Wang, D. Yan, D. W. Shaffer, X. Ye, B. H. Layne, J. J. Concepcion, M. Liu, C.-Y. Nam, *Chem. Mater.* **2018**, *30*, 324.

[8] A. Morais, C. Longo, J. R. Araujo, M. Barroso, J. R. Durrant, A. F. Nogueira, *Phys. Chem. Chem. Phys.* **2016**, *18*, 2608.

[9] C. Lee, D. Jeon, S. Bae, H. Kim, Y. Han, Y. W. Lee, J. Ryu, *ChemSusChem* **2018**, *11*, 3534.

[10] Z.-Q. Wei, X.-C. Dai, S. Hou, Y.-B. Li, M.-H. Huang, T. Li, S. Xu, F.-X. Xiao, *J. Mater. Chem. A* **2020**, *8*, 177.

[11] W. Fan, C. Chen, H. Bai, B. Luo, H. Shen, W. Shi, *Appl. Catal. B Environ.* **2016**, *195*, 9.

[12] D. Hidalgo, S. Bocchini, M. Fontana, G. Saracco, S. Hernández, *RSC Adv.* **2015**, *5*, 49429.

[13] D. M. Sanke, N. G. Ghosh, S. Das, H. S. Karmakar, A. Sarkar, S. S. Zade, *J. Colloid Interface Sci.* **2021**, *601*, 803.